

# Spin-Coated Polyelectrolyte Coacervate Films

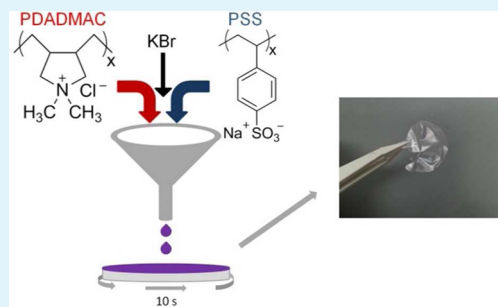
Kristopher D. Kelly and Joseph B. Schlenoff\*

Department of Chemistry and Biochemistry, Florida State University, Tallahassee, Florida 32306-4390, United States

## Supporting Information

**ABSTRACT:** Thin films of complexes made from oppositely charged polyelectrolytes have applications as supported membranes for separations, cell growth substrates, anticorrosion coatings, biocompatible coatings, and drug release media, among others. The relatively recent technique of layer-by-layer assembly reliably yields conformal coatings on substrates but is impractically slow for films with thickness greater than about 1  $\mu\text{m}$ , even when accelerated many fold by spraying and/or spin assembly. In the present work, thin, uniform, smooth films of a polyelectrolyte complex (PEC) are rapidly made by spin-coating a polyelectrolyte coacervate, a strongly hydrated viscoelastic liquidlike form of PEC, on a substrate. While the apparatus used to deposit the PEC film is conventional, the behavior of the coacervate, especially the response to salt concentration, is highly nontraditional. After glassification by immersion in water, spun-on films may be released from their substrates to yield free-standing membranes of thickness in the micrometer range.

**KEYWORDS:** layer by layer, LbL, multilayers, membrane, viscosity, separations



## INTRODUCTION

Polyelectrolyte complexes (PECs), either precipitated in bulk or adsorbed layer-by-layer (LbL) onto a surface (“polyelectrolyte multilayers”, PEMUs), have been driving numerous advances in engineering and technology in recent years.<sup>1–5</sup> The complex,  $\text{Pol}^+\text{Pol}^-$ , from complementary charges on negative,  $\text{Pol}^-$ , and positive,  $\text{Pol}^+$ , polyelectrolyte units can be reversibly broken by the addition of salt ions,  $\text{M}_{\text{aq}}^+$  and  $\text{A}_{\text{aq}}^-$ , as shown below.<sup>6,7</sup> Salt ions progressively transform intrinsic  $\text{Pol}^+\text{Pol}^-$  ion pairs to extrinsic sites, where the polymer repeat unit is compensated by a counterion.



A large library of polyelectrolytes,<sup>8</sup> positive or negative, natural or biological, hydrophobic or hydrophilic, some responsive to external stimuli,<sup>9</sup> some pH-dependent,<sup>10</sup> and cytophobic or cytophilic,<sup>11,12</sup> provides a unique class of materials that can be fine-tuned for a desired property or application<sup>13</sup> such as membranes,<sup>14–21</sup> nanocomposites,<sup>22,23</sup> and biological applications.<sup>24–27</sup> Surface chemistry and mechanical properties control how complexes interact with the local environment.

The multilayering, or LbL, method consistently produces thin, continuous, conformal coatings of PEC using simple aqueous processing methods.<sup>1,28,29</sup> A degree of “fuzzy” layering was demonstrated in some PEMUs.<sup>30</sup> A major practical drawback is the slow speed at which the coating method, which requires alternating immersion of the substrate into baths of polyelectrolytes, builds up the thin film. Some conditions or combinations of polymer, which yield more fluidlike PEMUs, grow faster because of the enhanced mobility of the constituents.<sup>31,32</sup> Using such “exponential” growth,<sup>33–35</sup> it is

possible to generate PEMUs on the order of a few microns within 10 or so layers. However, many combinations of polyelectrolytes grow “linearly” because they are below the glass transition temperature<sup>36</sup> of the complex. Such systems require dozens or hundreds of layers to reach micron thicknesses.

With the introduction of alternate spraying,<sup>37–39</sup> LbL deposition was accelerated considerably, and later engineering methods were refined to enable rapid, large-area coatings.<sup>39,40</sup> Other methods of accelerating the mass transport of polyelectrolyte to the surface include spinning the substrate face down in the polyelectrolyte solution (hydrodynamic LbL)<sup>41</sup> and spinning the substrate face up as solution is dropped or sprayed<sup>22,42</sup> on it. The latter “spin-assisted” LbL methods were shown to rapidly produce high-quality multilayers.<sup>22,43–46</sup>

All multilayering methods require intensive processing. Simultaneous spraying of positive and negative polyelectrolytes has been demonstrated,<sup>40,47</sup> but the process must be carefully controlled to yield 1:1 stoichiometry, which is approximated by multilayering, and to allow large quantities of excess solvent to drain from the film. Maintaining a 1:1 stoichiometry of polyelectrolyte repeat units in PEMUs, which was assumed to be controlled by the self-assembling nature of alternating adsorption,<sup>28</sup> turns out to be a significant problem for films thicker than a few layers. Because of the difference in mobility between the cation and anion,<sup>34</sup> a layer of extrinsic charge builds up within the PEMU.<sup>48</sup> This intrinsic charge leads to unforeseen inhomogeneities in the composition and properties

Received: April 6, 2015

Accepted: June 4, 2015

Published: June 16, 2015

of multilayers, including membrane transport and mechanical properties.

Early work by Michaels and co-workers described methods for dissolving PECs in strong ternary complexes of water, salt, and organic solvent.<sup>49,50</sup> These solutions, where polyelectrolyte chains are decoupled from each other, could be cast on plates to re-form complexes using conventional polymer film-casting techniques (i.e., pumping off the solvent). While casting is not rapid, it does provide a route to thick-film ( $>1\ \mu\text{m}$ ) morphologies of PECs for applications requiring thicker, free-standing material. Bixler and Michaels<sup>51</sup> evaluated the performance of cast PEC films for purifying salty water by reverse osmosis.

Polyelectrolyte coacervates (PECOVs)<sup>52–55</sup> represent an interesting intermediate between PECs and solutions of the same polyelectrolytes (i.e., where all polymer chains are isolated). These coacervates contain weakly bound polyelectrolytes that are so well hydrated that they behave like fluids. At the same time, the remaining physical interactions impart elastic properties.<sup>55</sup> These interactions are a mix of classical polymer entanglements and “sticky” ion pairings.<sup>56</sup> There has been a recent surge of interest in PECOVs, first described by Bungenberg de Jong and Kruyt around 1930 while investigating biocolloidal systems,<sup>57</sup> because they mimic the elastic fluidlike properties of many biological systems.<sup>58</sup> Research on the practical aspects of coacervates has been accompanied by fundamental studies of their properties. We recently explored the spectrum of properties controlled by salt (KBr) concentration, as in eq 1, in a PEC made from poly(styrenesulfonate) (PSS) and poly(diallyldimethylammonium chloride) (PDADMAC).<sup>56</sup> With increasing salt content (0–1.4 M KBr), a PSS/PDADMA PEC is transformed from a tough to a rubbery polymer. Then, over a narrow range of KBr concentration (1.4–1.8 M), the material behaves like a coacervate. At 1.8 M, the coacervate dissociates to yield individual chains (i.e., a true solution of polyelectrolytes).<sup>56</sup>

The goal of the present work was to exploit the liquidlike properties of PSS/PDADMA coacervates to form a thin film on a substrate by spin-coating. Spin coating is widely used by industry for rapidly producing a thin polymer film of thickness  $>1\ \mu\text{m}$  on a surface.<sup>59</sup> For example, semiconductor processing (“chip” making) requires several spun-on coatings of polymers. Although several counterintuitive properties were discovered, spun-on coatings from coacervates and dissolved PEC solutions were efficiently produced and released from their substrate. Spinning coacervate is more efficient at producing thicker stoichiometric films than similar strategies, such as LbL, spraying, and spin-assisted LbL buildups.

## EXPERIMENTAL SECTION

**Materials.** Poly(diallyldimethylammonium chloride) (PDADMAC; Onco-Nalco, SD 46104; molar mass  $400000\ \text{g mol}^{-1}$ ), poly(4-styrenesulfonic acid, sodium salt) (PSS; AkzoNobel, VERSA TL130; molar mass  $200000\ \text{g mol}^{-1}$ ), and potassium bromide (KBr; Sigma-Aldrich) were used as received from the manufacturer. Poly(ether sulfone) (PES) membranes (25-mm-diameter Supor-100  $0.1\ \mu\text{m}$  filters,  $130\ \mu\text{m}$  thick) were from PALL Life Sciences. All salt solutions were prepared using  $18\ \text{M}\Omega$  deionized water (Barnstead E-pure).

**PEC Preparation.** PECs were produced by the simultaneous mixing of 1.0 L aqueous solutions of 0.125 M PDADMAC and PSS each in 0.25 M NaCl with stirring for 30 min.<sup>3</sup> After the white precipitate was allowed to form, the excess salt/water mixture was decanted and the precipitate hand-squeezed to remove as much liquid as possible. The remaining white crumbled aggregate was broken into

pieces of about 1 cm across and washed with copious amounts of water for 3 days to remove all residual NaCl. The PEC was then dried in an oven at  $120\ ^\circ\text{C}$ . The dried complex was a tough translucent orange solid, which was then ground to a fine powder in a coffee grinder.

**PECOV Preparation.** Following our earlier protocol,<sup>56</sup> 1.5 g of a dry PEC powder was added to a 25 mL vial with a desired amount of 2.5 M KBr depending on the final KBr concentration. After a few days when the complex has dissolved,  $18\ \text{M}\Omega$  water was added to a total volume of 15 mL to re-form the coacervate. This “backwards” method was preferred to adding PEC to the desired [KBr], which takes significantly longer to produce coacervate. KBr was chosen over NaCl as the salt to make coacervates because of its ability to dope the complex more efficiently. Mixtures containing [KBr]  $\geq 1.8\ \text{M}$  were in the solution phase, while 1.4–1.8 M KBr provided the coacervate phase.<sup>56</sup> All experiments were performed at room temperature.

**Spin Coating.** Thin films were prepared using a Chemat KW-4A spin coater. Aliquots of  $250\ \mu\text{L}$  were dispensed onto 18-mm-diameter glass coverslips prior to acceleration to 1000–6000 rpm for 5–60 s for spreading to create a range of films with varying thickness and roughness profiles. To make removable intact films, coacervates were spun onto 18-mm-diameter mirror-polished aluminum disks treated with 0.1 M NaOH for 5 s to render them more wettable. Each film on its substrate was then removed from the spin coater and rinsed in  $18\ \text{M}\Omega$  water three times for 1 min each to extract KBr.

**Profilometry.** A Tencor Alpha-Step 200 profilometer was used to measure the thickness. A  $5\ \mu\text{m}$  stylus scanned across the surface of the film at a rate of  $10\ \mu\text{m s}^{-1}$  for 40 s, yielding a line profile of the sample with a z-resolution of 5 nm. To measure the film thickness, a scratch was made down to the substrate using a single-side razor blade. Thickness measurements were collected every 2 mm from the edge of an 18-mm glass disk, with a scratch exactly in the center for a total of five thickness measurements per sample using this step-edge method.

**Radiolabeling.** A released PECO film made from 1.7 M KBr was soaked in 0.2 M NaCl for 18 h and then washed and stored in  $18\ \text{M}\Omega$  water for 2 h. The film was then dried and placed in a  $^{125}\text{I}^-$  solution ( $1.25\ \text{Ci mol}^{-1}$ ,  $10^{-3}\ \text{M}$ ) to measure the anion content or  $^{22}\text{Na}^+$  ( $4.5\ \text{Ci mol}^{-1}$ ,  $10^{-4}\ \text{M}$ ) to measure the sodium ( $\text{Na}^+$ ) content, for 2 h. After rinsing and drying, scintillation counting was performed using a plastic scintillator and a photomultiplier tube as described previously.<sup>48</sup>

**Atomic Force Microscopy (AFM).** The surface topology of spun PEC films was acquired using a MFP-3D atomic force microscope (Asylum Research Inc., Santa Barbara, CA), equipped with an ARC2 controller, *IgorPro* software, and silicon AC240-TS probes (Olympus; radius =  $9 \pm 2\ \text{nm}$ , height =  $14 \pm 2\ \mu\text{m}$  on aluminum-coated cantilevers with a spring constant of  $2\ \text{N m}^{-1}$ ). The alternating-current mode was employed to determine the topography of PEC films made with a range of spin parameters. The cantilever was tuned to 10% below its resonance frequency with scan sizes of  $5 \times 5$ ,  $10 \times 10$ , and  $20 \times 20\ \mu\text{m}$  at a scan rate of 1.0 Hz. The root-mean-square (rms) roughness of the surface was collected on four  $5 \times 5\ \mu\text{m}$  areas on each sample and averaged.

**Scanning Electron Microscopy (SEM).** A JSM-7401f ultrahigh-resolution (resolution 1.5 nm at 1 kV) field-emission scanning electron microscope equipped with a strongly excited low-aberration conical lens and cold-field tungsten single-crystal emitter was used to image the surface of PEC films spun from 1.7 and 1.9 M KBr at 3000 rpm for 10, 15, and 20 s.

**Mechanical Tests.** Coacervate from 1.7 M KBr was spun onto 1-in.-diameter aluminum-foil-covered silica disks at 3000 rpm. These larger samples were removed with a brief soak in 0.1 M NaOH. Rectangles of dimensions  $20\ \text{mm} \times 3\ \text{mm} \times 10\ \mu\text{m}$  were cut and mounted on a Thümler TH2730 tensile testing machine equipped with a 3 kN load cell and strained to 2% at a rate of  $7\ \text{mm min}^{-1}$ .

## RESULTS AND DISCUSSION

Spin coating is practiced widely to rapidly deposit a thin coating on a substrate.<sup>59,60</sup> Here, the use of water instead of volatile organics as a solvent provides a “green” processing method. This work employs stoichiometric (1:1) complexes of PSS and

PDADMA, which have been transformed to near-stoichiometric coacervates with the addition of sufficient KBr solution. Prior extensive investigations of PSS/PDADMA coacervates show that they are produced over the [KBr] range of 1.4–1.80 M.<sup>56</sup> While any combination of positive and negative polyelectrolyte potentially forms coacervates, the salt type and concentration must be optimized for each combination. At concentrations greater than 1.80 M KBr, the solution contains dissolved (separated) polyelectrolyte chains. Because these chains are at a dense concentration (higher than the critical overlap concentration), the viscosity of the dissolved solution (50–100 cP) is still significantly greater than that of water (1 cP). Films were obtained by spin-coating coacervate or dissolved PEC, and the films were solidified by immersion in water, which rapidly extracts the salt, instead of drying. However, the coacervate system provided fascinating, unexpected, and nontraditional responses to variables such as the spin time and speed.

Spin coating is typically characterized by at least four regimes:<sup>59,60</sup> dispensing, where an aliquot of solution is placed on the substrate; “spin up”, where the solution is spread out at relatively low rpm; “spin out”, where the rpm increases and excess solution is flung off the substrate; and evaporation, where the film dries while spinning. Evaporation actually occurs throughout and therefore overlaps with the other steps. In the limit of no evaporation, Emslie et al. determined the thickness,  $h$ , of the liquid film at any distance  $r_o$  from the center:<sup>61</sup>

$$h = \frac{h_0}{(1 + 4Kh_0^2t)^{0.5}}$$

$$K = \frac{\rho\omega^2}{3\eta} \quad (2)$$

where  $t$  is the spin time,  $\omega$  is the angular velocity, and  $\eta$  is the viscosity. The initial thickness of the fluid layer is represented by  $h_0$ , which is independent of  $r_o$ . Including evaporation while spinning/thinning yields more complex predictions, especially if the viscosity changes with drying (as is inevitable with polymer solutions). Equation 2 shows that, because a thick layer thins significantly faster than a thin one, there will be a tendency for uniformity. The thickness increases with viscosity and decreases with spin time.

Good-quality PEC films spun from coacervate on glass disks could not be obtained with standard spin-coating protocols employed for solutions of polymers in volatile solvents. For example, poly(methyl methacrylate) in toluene can produce a uniform thin film at 3000 rpm for 60 s,<sup>60</sup> whereas coacervate created an uneven morphology under the same conditions. With coacervate in aqueous solutions, there was an appropriate spin time at a specific spin velocity to generate a uniformly thick film without the production of either a “dish” (thinner in the middle) or “dome” (thicker in the middle) morphology. After the film was spun, it was rinsed in water to remove KBr and to rapidly transform the coacervate into a salt-free, glassy PEC.<sup>56</sup> An estimate of the time taken,  $t$ , for the transformation of a coacervate film into a salt-free film is made using a diffusion coefficient,  $D$ , of  $8 \times 10^{-7} \text{ cm}^2 \text{ s}^{-1}$  for NaBr in PSS/PDADMA<sup>7</sup> using  $\Delta = (2Dt)^{1/2}$ . A  $\Delta = 10\text{-}\mu\text{m}$ -thick film would lose most of its ions within 0.6 s.

It was found that short spin times with immediate ramping to the maximum spin speed and then stopping (no ramp down) produced the best (most uniform) liquid films, which could be

classified to solid films by immersion in water. The unusual behavior of coacervates in spin coating is immediately seen by the thicknesses and profiles in Figure 1. The thickness did not

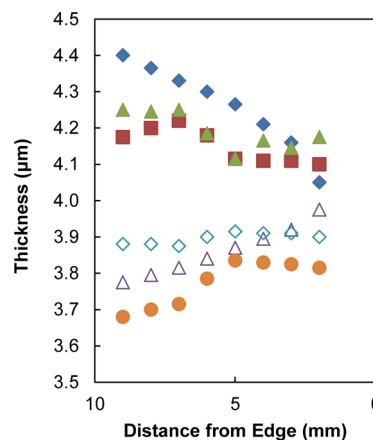


**Figure 1.** Dome versus dish morphology of spun coacervate films. PSS/PDADMA coacervates in 1.7 M KBr spun on 18-mm-diameter glass disks for (blue  $\blacklozenge$ ) 5 s, (red  $\blacksquare$ ) 10 s, (green  $\blacktriangle$ ) 20 s, (blue  $\triangle$ ) 30 s, (blue  $\diamond$ ) 45 s, and (orange  $\bullet$ ) 60 s. All samples were produced at a spin speed of 5000 rpm.

decrease much with spinning time, as eq 2 predicted. Also, short times produced a “dome” effect of slightly thicker films toward the center of the sample, an indication of insufficient thinning time. However, additional spin time resulted in an atypical “dish” profile, where material at the center is thinner.

The viscosity of PECOVs depends on the salt concentration. The lower the salt concentration the more “sticky” ion pairs there are between polymer chains (according to eq 1) and, therefore, the higher the viscosity. For our PSS/PDADMA coacervates at room temperature, the viscosity  $\eta$  is a strong nonlinear function of the concentration of KBr over the range  $1.3 \text{ M} < [\text{KBr}] < 1.8 \text{ M}$  [see the Supporting Information (SI) for data adapted from ref 56]:

$$\eta \text{ (cP)} = \frac{1.5 \times 10^9}{[\text{KBr}]^{28}} \quad (3)$$

A small increase in [KBr] leads to a substantial decrease in the viscosity; i.e., the liquid becomes less viscous as the water evaporates. The decrease in the viscosity led to a buildup near the edge of the film (“dish” morphology) as the water started to evaporate, but the variations in the thickness across the film amounted to less than 5% of the film thickness (Figure 1).

The confounding behavior of spin-coated coacervates is further demonstrated in Figure 2, where comparisons are made with dissolved PEC (in 1.9 M KBr). The combined effects of spin time and speed are shown in a 3D plot. Again, almost no influence of the spin time is seen for the coacervate. The thickness remains fairly constant at lower rpm but drops quickly at the highest rpm values. In contrast, the dissolved PEC thins as both the time and rpm increase. The same data are shown as 2D plots in the SI.

For PEC in 1.7 M KBr, which exhibits a viscosity of 300 cP,<sup>56</sup> ion-pair interactions between polyelectrolyte chains are still abundant and prevent rapid spreading of coacervates during spinning. In 1.8 M KBr, all of the ion pairs between polyelectrolytes are broken,<sup>56</sup> so when the concentration of KBr increased to 1.9 M, which had a viscosity of 70 cP,

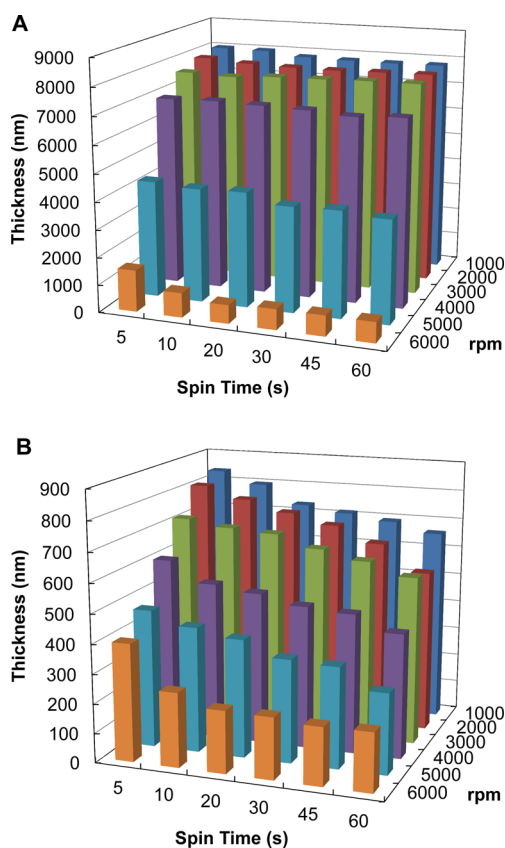


**Figure 2.** Thickness of spun films of PSS/PDADMA PEC from the coacervate in 1.7 M KBr (A) and the solution in 1.9 M KBr (B) as a function of the spinning speed and time.

polyelectrolyte chains flowed more freely past one another, which decreased the thickness to less than 1  $\mu\text{m}$ .

The composition of films spin-coated on double-side polished silicon wafers was verified with FTIR spectroscopy. Figure 3 shows the comparison of spectra of a 690 nm PEC film spun from a 1.9 M KBr PEC film and a 570 nm 40-layer film made from multilayering that was known to be stoichiometric in PSS and PDADMA.<sup>62</sup> Subtraction of the spectra of multilayered PEC from spun PEC (after scaling the PEMU spectrum to account for a small difference in thickness) revealed no residual signal from the PSS bands (1008 and 1033  $\text{cm}^{-1}$ ) and PDADMA band (1475  $\text{cm}^{-1}$ ), showing that both methods of producing films yield material with equivalent amounts of each polymer. Films spun from 1.7 M KBr were too thick and yielded excessive absorbance values that fell outside of the linear response of absorbance to thickness (Beer's law).

Although the comparison of FTIR spectra in Figure 3 indicates stoichiometric quantities of PSS and PDADMA, it is not accurate to better than 5% and cannot exclude the presence of ions. If a PEC membrane is to be used for selective ion transport, a small but persistent population of fixed ion-exchange sites ("extrinsic" compensation) may influence the selectivity and permeability of the membrane. In order to determine the ion content with greater accuracy, membranes of spun PEC were probed with radiolabeled iodide and sodium. A PEC film spun from 1.7 M KBr (mass 3.5 mg) was released using the technique described below. The film was rinsed in either  $^{125}\text{I}^-$  or  $^{22}\text{Na}^+$  to determine its ion content by exchanging radiolabeled with unlabeled ions within the film.<sup>7</sup> From the mass of the film and a density of 1.27  $\text{g cm}^{-3}$ , the amount of

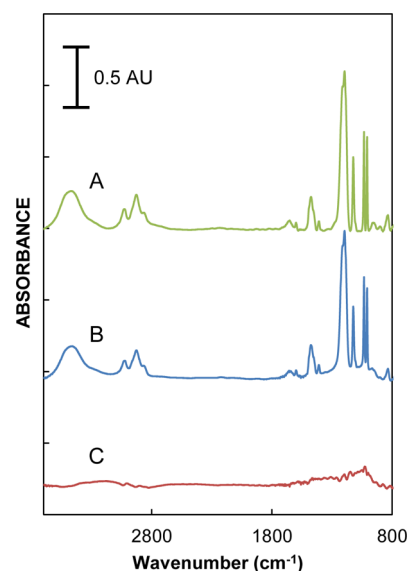


**Figure 3.** FTIR transmission spectra of (A) a PSS/PDADMA film spun from 1.9 M KBr (690 nm) and (B) a 40-layer stoichiometric PDADMA/PSS multilayer (570 nm) both on silicon wafers. (C) Difference spectrum.

PSS and PDADMA groups was estimated to be 11.4  $\mu\text{mol}$ . Scintillation counting with  $^{125}\text{I}^-$  to probe positive extrinsic charge showed  $1.26 \times 10^{-3}$   $\mu\text{mol}$  of excess PDADMA( $\text{Cl}^-$ ). Similar experiments with  $^{22}\text{Na}^+$  showed 6.54  $\mu\text{mol}$  of excess PSS( $\text{Na}^+$ ). These results translate to an anion content of 0.0011 mol % and a cation content of 0.57 mol % within the PEC film; i.e., the ratio of PSS/PDADMA is 1.0057:1.0000, close to 1:1. The slight excess of PSS is consistent with the finding that the PSS/PDADMA starting coacervate has a slight excess of PSS.<sup>56</sup>

Most films of PEC deposited by the multilayering procedure exhibit surface roughness,<sup>1</sup> a morphological feature that would not be a serious issue for membrane permeability but would present problems for maintaining a clean (unfouled) surface. In addition, applications relying on smooth films, such as pattern formation, would be compromised. The amount of roughness acquired during multilayer buildup is often observed to scale approximately with the thickness of the film. For PSS/PDADMA multilayers, rms roughness on the order of 20% of the film thickness is observed.<sup>63</sup> Extending the rationale for changes in the surface topography in swollen gels,<sup>64,65</sup> it is believed that roughness results from significant volume changes due to variations in the water content in the film, depending on the "last-added" layer.<sup>63</sup> The PSS/PDADMA coacervates used here have substantial (>60 wt %) water,<sup>56</sup> which would lead to large volume changes as both salt and water leave the PEC.

AFM images were recorded on the surface of rinsed and dried PEC films from 1.7 and 1.9 M KBr produced at 3000 rpm for 10 s to determine roughness, as shown in Figure 4. Over surface areas of  $20 \times 20$  and  $5 \times 5$   $\mu\text{m}$ , the roughnesses of PEC films from 1.7 M KBr were 16 and 4 nm, respectively. For PEC from 1.9 M KBr, the roughnesses were 13 and 8 nm for the same scales, showing that both films are relatively smooth (less than 0.1% of the film thickness). Such a low level of roughness was surprising but encouraging, given the findings with thick multilayers of PSS/PDADMA.<sup>63</sup> It is probable that, upon immersion in water, KBr continues to plasticize the spun-coated film as it leaves the PEC, relieving the stresses on the material and preventing deformation.

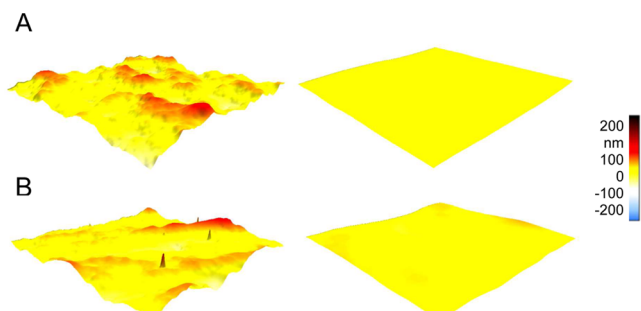


**Figure 4.** AFM images of PEC films spun from PSS/PDADMA with 1.7 M KBr (A) and 1.9 M KBr (B). XY scan range of  $20 \times 20 \mu\text{m}$  on the left and  $5 \times 5 \mu\text{m}$  on the right. The rms roughness for (A) 4 nm on the  $20 \times 20 \mu\text{m}$  scan and 1.1 nm in the  $5 \times 5 \mu\text{m}$  scan and (B) 13 and 8 nm, respectively.

To further evaluate the topology, SEM was performed for films deposited from 1.7 and 1.9 M KBr under the same conditions as those used for the AFM studies. SEM (Figure 5)

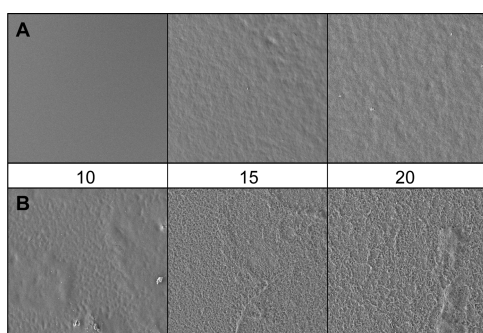


**Figure 5.** SEM images ( $20 \times 20 \mu\text{m}$ ) of PEC films from 1.7 (upper row A) and 1.9 M KBr (lower row B). Time in seconds is shown between panels. The surface topography varies with the spin speed, as shown by the rougher terrain exhibited for longer spin times. Evaporation of water during longer spin times is thought to drive microphase separation, which produces rougher films.

showed increased roughness with longer spin times, observations also made with AFM. This roughness evolved quite rapidly and is counterintuitive under the assumption that strong centrifugal fields should smooth surfaces out. On the other hand, increasing roughness, or at least texturing, is consistent with microphase separations widely observed in coacervates.<sup>52,53,66</sup> For the present system, small departures in temperature or salt concentration from the conditions under which a coacervate has been equilibrating yield microphase separation<sup>56</sup> as the material adjusts to a new equilibrium composition in the phase diagram.

Mirror-polished 18 mm aluminum disks were used as substrates for removable membranes. Coacervate did not wet the as-supplied aluminum (alloy 6061) disks efficiently, which led to poor-quality spun films. To promote wetting and adhesion of coacervate to the aluminum, each substrate was rinsed in 0.1 M NaOH, which allowed uniform spreading during spinning. A study of the film thickness on aluminum substrates as a function of the spinning time using 1.7 M KBr coacervate is shown in Figure 6. The 1.7 M coacervate was chosen over the 1.9 M solution to provide thicker films. In order to release films from aluminum disks, heat was applied via a 250 W heat lamp at a distance of 25 cm from the sample, which heated the substrate to  $60 \text{ }^\circ\text{C}$  and released films (due to

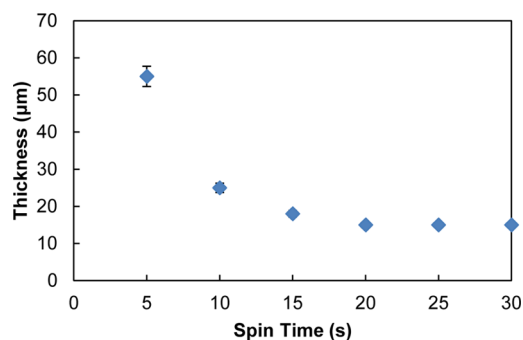


**Figure 6.** Thickness of the PEC films from 1.7 M KBr coacervate spun on a polished aluminum disk at 1000 rpm. Thickness versus spin time ( $\diamond$ ). Polished aluminum disks were used in place of glass to facilitate the release of PEC films.

shrinkage) after 30 min. This mild heat treatment did not change the polyelectrolytes, as judged by FTIR spectroscopy. Thermal gravimetric analysis shows that PSS/PDADMA multilayers are stable up to about  $300 \text{ }^\circ\text{C}$ .<sup>67</sup> As an alternative release method, 0.1 M NaOH was able to gently dissolve some of the substrate under films, which could be peeled, still wet, from the substrate. Released films are optically transparent, as seen in Figure 7. The thickness of the films was measured either



**Figure 7.** Standalone PEC film (1 inch diameter and  $15 \mu\text{m}$  thickness) spun from PSS/PDADMA coacervate in 1.7 M KBr at 1000 rpm.

with a digital micrometer or by weighing the film, measuring the area, and determining the thickness using the density. These methods were within 10% of each other. Films spun from 1.7 M KBr on larger aluminum disks (1 in. diameter) were released with NaOH and subjected to tensile testing under ambient conditions (see the SI for stress–strain curves). Stress relaxation experiments (see the SI) showed the equilibrium modulus to be 1050 MPa and the tensile strength about 50 MPa under ambient conditions ( $23 \text{ }^\circ\text{C}$  and 44% relative humidity).

It was observed that films spun under identical conditions from identical coacervates were somewhat thicker on the aluminum substrate than on clean glass (for example, compare Figures 6 and 2A). The reason for this difference is not yet understood but may stem from the difference in wetting on the two substrates and the elastic properties of the coacervate. However, the  $15\text{-}\mu\text{m}$ -thick film, produced in less than a minute, was flexible and rugged enough to handle and would be suitable

for use as a membrane supported by a wire mesh. For comparison, to produce films of PSS/PDADMA with this thickness via multilayering in 1 M NaCl with 5 min per layer and 30 s rinse steps (about 15 nm per layer<sup>41</sup>) would take about 300 h and even spraying at 30 s per layer would take about 20 h.<sup>38,68</sup> There is no reason to expect structure within a spin-coated coacervate film, whereas “fuzzy” laying is possible in multilayered films.<sup>1</sup> As an example of supported membranes, films were spun from 1.7 and 1.9 M KBr onto porous PES, yielding uniform PEC films of thickness 11 and 2  $\mu\text{m}$ , respectively.

## CONCLUSIONS

With the introduction of a technique to rapidly deposit films of PEC of the appropriate thickness for supported membranes for separations, many of the membrane applications discussed in the literature may be implemented more easily. It should also be possible to make defect-free PEC films on porous and nonporous substrates/supports by dip-coating or spin-coating these substrates with coacervates. Within a coacervate, the density of the chains is high enough to exceed the critical chain overlap concentration, which allows the PEC in the coacervate to collapse as a continuous sheet in rinsewater when the salt leaves it rather than disintegrate into particles.<sup>69</sup> Starting materials for coacervate formation are prepared from the constituent polyelectrolytes by complexing polyanions and polycations in bulk with added salt. The concentration of salt required to achieve the desired viscosity depends on the identity of the polyelectrolytes and salt, with the latter following a Hofmeister series.<sup>7,54</sup> Processing is done with all-aqueous systems, providing an environmentally friendlier route to polymer film formation.

## ASSOCIATED CONTENT

### Supporting Information

Optical microscopy images of spin-coated films, viscosity versus salt concentration over the range of 1.25–1.78 M KBr, 2D plots of the thickness versus spinning speed or time, theoretical thickness using eq 2, and stress–strain curves for membrane tensile tests. The Supporting Information is available free of charge on the ACS Publications website at DOI: 10.1021/acsami.5b02988.

## AUTHOR INFORMATION

### Corresponding Author

\*E-mail: schlen@chem.fsu.edu.

### Notes

The authors declare no competing financial interest.

## ACKNOWLEDGMENTS

The authors acknowledge Qifeng Wang for help in SEM and Hadi Fares for radiolabeling studies. This work was supported by Grant DMR 1207188 from the National Science Foundation.

## REFERENCES

- (1) Decher, G.; Schlenoff, J. B. *Multilayer Thin Films: Sequential Assembly of Nanocomposite Materials*, 2nd ed.; Wiley-VCH: Weinheim, Germany, 2012.
- (2) Müller, M. *Polyelectrolyte Complexes in the Dispersed and Solid State II: Applications*; Springer: Berlin, 2014; Vol. 256.
- (3) Shamoun, R. F.; Reisch, A.; Schlenoff, J. B. Extruded Saloplastic Polyelectrolyte Complexes. *Adv. Funct. Mater.* **2012**, *22*, 1923–1931.

(4) Gribova, V.; Auzely-Velty, R.; Picart, C. Polyelectrolyte Multilayer Assemblies on Materials Surfaces: From Cell Adhesion to Tissue Engineering. *Chem. Mater.* **2012**, *24*, 854–869.

(5) Zhao, Q.; An, Q. F. F.; Ji, Y. L.; Qian, J. W.; Gao, C. J. Polyelectrolyte Complex Membranes for Pervaporation, Nanofiltration and Fuel Cell Applications. *J. Membr. Sci.* **2011**, *379*, 19–45.

(6) Farhat, T. R.; Schlenoff, J. B. Doping-Controlled Ion Diffusion in Polyelectrolyte Multilayers: Mass Transport in Reluctant Exchangers. *J. Am. Chem. Soc.* **2003**, *125*, 4627–4636.

(7) Ghostine, R. A.; Shamoun, R. F.; Schlenoff, J. B. Doping and Diffusion in an Extruded Saloplastic Polyelectrolyte Complex. *Macromolecules* **2013**, *46*, 4089–4094.

(8) Bertrand, P.; Jonas, A.; Laschewsky, A.; Legras, R. Ultrathin Polymer Coatings by Complexation of Polyelectrolytes at Interfaces: Suitable Materials, Structure and Properties. *Macromol. Rapid Commun.* **2000**, *21*, 319–348.

(9) Addison, T.; Cayre, O. J.; Biggs, S.; Armes, S. P.; York, D. Incorporation of Block Copolymer Micelles into Multilayer Films for Use as Nanodelivery Systems. *Langmuir* **2008**, *24*, 13328–13333.

(10) Shiratori, S. S.; Rubner, M. F. pH-Dependent Thickness Behavior of Sequentially Adsorbed Layers of Weak Polyelectrolytes. *Macromolecules* **2000**, *33*, 4213–4219.

(11) Thompson, M. T.; Berg, M. C.; Tobias, I. S.; Rubner, M. F.; Van Vliet, K. J. Tuning Compliance of Nanoscale Polyelectrolyte Multilayers to Modulate Cell Adhesion. *Biomaterials* **2005**, *26*, 6836–6845.

(12) Mendelsohn, J. D.; Yang, S. Y.; Hiller, J.; Hochbaum, A. I.; Rubner, M. F. Rational Design of Cytophilic and Cytophobic Polyelectrolyte Multilayer Thin Films. *Biomacromolecules* **2003**, *4*, 96–106.

(13) Ariga, K.; Yamauchi, Y.; Rydzek, G.; Ji, Q.; Yonamine, Y.; Wu, K. C. W.; Hill, J. P. Layer-by-layer Nanoarchitectonics: Invention, Innovation, and Evolution. *Chem. Lett.* **2014**, *43*, 36–68.

(14) Fadhillah, F.; Zaidi, S. M. J.; Khan, Z.; Khaled, M.; Rahman, F.; Hammond, P. Development of Multilayer Polyelectrolyte Thin-film Membranes Fabricated by Spin Assisted Layer-by-Layer Assembly. *J. Appl. Polym. Sci.* **2012**, *126*, 1468–1474.

(15) Stroeve, P.; Vasquez, V.; Coelho, M. A. N.; Rabolt, J. F. Gas Transfer in Supported Films Made by Molecular Self-assembly of Ionic Polymers. *Thin Solid Films* **1996**, *285*, 708–712.

(16) Krasemann, L.; Tieke, B. Ultrathin Self-assembled Polyelectrolyte Membranes for Pervaporation. *J. Membr. Sci.* **1998**, *150*, 23–30.

(17) Harris, J. J.; Stair, J. L.; Bruening, M. L. Layered Polyelectrolyte Films as Selective, Ultrathin Barriers for Anion Transport. *Chem. Mater.* **2000**, *12*, 1941–1946.

(18) Toutianoush, A.; Schnepf, J.; El Hashani, A.; Tieke, B. Selective Ion Transport and Complexation in Layer-by-Layer Assemblies of *p*-Sulfonato-calix[*n*]arenes and Cationic Polyelectrolytes. *Adv. Funct. Mater.* **2005**, *15*, 700–708.

(19) Argun, A. A.; Ashcraft, J. N.; Hammond, P. T. Highly Conductive, Methanol Resistant Polyelectrolyte Multilayers. *Adv. Mater.* **2008**, *20*, 1539–1543.

(20) Cheng, C.; Yaroshchuk, A.; Bruening, M. L. Fundamentals of Selective Ion Transport through Multilayer Polyelectrolyte Membranes. *Langmuir* **2013**, *29*, 1885–1892.

(21) Joseph, N.; Ahmadiannamini, P.; Hoogenboom, R.; Vankelecom, I. F. J. Layer-by-layer Preparation of Polyelectrolyte Multilayer Membranes for Separation. *Polym. Chem.* **2014**, *5*, 1817–1831.

(22) Merrill, M. H.; Sun, C. T. Fast, Simple and Efficient Assembly of Nanolayered Materials and Devices. *Nanotechnology* **2009**, *20*, 075606.

(23) Fu, J.; Wang, Q.; Schlenoff, J. B. Extruded Superparamagnetic Saloplastic Polyelectrolyte Nanocomposites. *ACS Appl. Mater. Interfaces* **2014**, *7*, 895–901.

(24) Lichter, J. A.; Van Vliet, K. J.; Rubner, M. F. Design of Antibacterial Surfaces and Interfaces: Polyelectrolyte Multilayers as a Multifunctional Platform. *Macromolecules* **2009**, *42*, 8573–8586.

- (25) Porcel, C. H.; Schlenoff, J. B. Compact Polyelectrolyte Complexes: "Saloplastic" Candidates for Biomaterials. *Biomacromolecules* **2009**, *10*, 2968–2975.
- (26) Hariri, H. H.; Schlenoff, J. B. Saloplastic Macroporous Polyelectrolyte Complexes: Cartilage Mimics. *Macromolecules* **2010**, *43*, 8656–8663.
- (27) Boudou, T.; Crouzier, T.; Ren, K. F.; Blin, G.; Picart, C. Multiple Functionalities of Polyelectrolyte Multilayer Films: New Biomedical Applications. *Adv. Mater.* **2010**, *22*, 441–467.
- (28) Decher, G. Fuzzy Nanoassemblies: Toward Layered Polymeric Multicomposites. *Science* **1997**, *277*, 1232–1237.
- (29) Hammond, P. T. Recent Explorations in Electrostatic Multilayer Thin Film Assembly. *Curr. Opin. Colloid Interface Sci.* **1999**, *4*, 430–442.
- (30) Schmitt, J.; Grünewald, T.; Decher, G.; Pershan, P. S.; Kjaer, K.; Lösche, M. Internal Structure of Layer-by-Layer Adsorbed Polyelectrolyte Films—a Neutron and X-Ray Reflectivity Study. *Macromolecules* **1993**, *26*, 7058–7063.
- (31) Lavalle, P.; Picart, C.; Mutterer, J.; Gergely, C.; Reiss, H.; Voegel, J. C.; Senger, B.; Schaaf, P. Modeling the Buildup of Polyelectrolyte Multilayer Films Having Exponential Growth. *J. Phys. Chem. B* **2004**, *108*, 635–648.
- (32) Xu, L.; Pristiniski, D.; Zhuk, A.; Stoddart, C.; Ankner, J. F.; Sukhishvili, S. A. Linear versus Exponential Growth of Weak Polyelectrolyte Multilayers: Correlation with Polyelectrolyte Complexes. *Macromolecules* **2012**, *45*, 3892–3901.
- (33) Elbert, D. L.; Herbert, C. B.; Hubbell, J. A. Thin Polymer Layers Formed by Polyelectrolyte Multilayer Techniques on Biological Surfaces. *Langmuir* **1999**, *15*, 5355–5362.
- (34) Picart, C.; Mutterer, J.; Richert, L.; Luo, Y.; Prestwich, G. D.; Schaaf, P.; Voegel, J. C.; Lavalle, P. Molecular Basis for the Explanation of the Exponential Growth of Polyelectrolyte Multilayers. *Proc. Natl. Acad. Sci. U.S.A.* **2002**, *99*, 12531–12535.
- (35) Kujawa, P.; Moraille, P.; Sanchez, J.; Badia, A.; Winnik, F. M. Effect of Molecular Weight on the Exponential Growth and Morphology of Hyaluronan/Chitosan Multilayers: A Surface Plasmon Resonance Spectroscopy and Atomic Force Microscopy Investigation. *J. Am. Chem. Soc.* **2005**, *127*, 9224–9234.
- (36) Shamoun, R. F.; Hariri, H. H.; Ghostine, R. A.; Schlenoff, J. B. Thermal Transformations in Extruded Saloplastic Polyelectrolyte Complexes. *Macromolecules* **2012**, *45*, 9759–9767.
- (37) Dubas, S. T.; Schlenoff, J. B. Polyelectrolyte Multilayers Containing a Weak Polyacid: Construction and Deconstruction. *Macromolecules* **2001**, *34*, 3736–3740.
- (38) Izquierdo, A.; Ono, S. S.; Voegel, J. C.; Schaaf, P.; Decher, G. Dipping versus Spraying: Exploring the Deposition Conditions for Speeding Up Layer-by-Layer Assembly. *Langmuir* **2005**, *21*, 7558–7567.
- (39) Krogman, K. C.; Zacharia, N. S.; Schroeder, S.; Hammond, P. T. Automated Process for Improved Uniformity and Versatility of Layer-by-Layer Deposition. *Langmuir* **2007**, *23*, 3137–3141.
- (40) Schaaf, P.; Voegel, J.-C.; Jierry, L.; Boulmedais, F. Spray-Assisted Polyelectrolyte Multilayer Buildup: from Step-by-Step to Single-Step Polyelectrolyte Film Constructions. *Adv. Mater.* **2012**, *24*, 1001–1016.
- (41) Dubas, S. T.; Schlenoff, J. B. Factors Controlling the Growth of Polyelectrolyte Multilayers. *Macromolecules* **1999**, *32*, 8153–8160.
- (42) Salomäki, M.; Peltonen, T.; Kankare, J. Multilayer Films by Spraying on Spinning Surface—Best of Both Worlds. *Thin Solid Films* **2012**, *520*, 5550–5556.
- (43) Chiarelli, P. A.; Johal, M. S.; Casson, J. L.; Roberts, J. B.; Robinson, J. M.; Wang, H. L. Controlled Fabrication of Polyelectrolyte Multilayer Thin Films Using Spin-Assembly. *Adv. Mater.* **2001**, *13*, 1167–1171.
- (44) Cho, J.; Char, K.; Hong, J. D.; Lee, K. B. Fabrication of Highly Ordered Multilayer Films Using a Spin Self-Assembly Method. *Adv. Mater.* **2001**, *13*, 1076–1078.
- (45) Lee, S. S.; Lee, K. B.; Hong, J. D. Evidence for Spin Coating Electrostatic Self-Assembly of Polyelectrolytes. *Langmuir* **2003**, *19*, 7592–7596.
- (46) Patel, P. A.; Dobrynin, A. V.; Mather, P. T. Combined Effect of Spin Speed and Ionic Strength on Polyelectrolyte Spin Assembly. *Langmuir* **2007**, *23*, 12589–12597.
- (47) Porcel, C. H.; Izquierdo, A.; Ball, V.; Decher, G.; Voegel, J. C.; Schaaf, P. Ultrathin Coatings and Poly(glutamic acid)/polyallylamine Films Deposited by Continuous and Simultaneous Spraying. *Langmuir* **2005**, *21*, 800–802.
- (48) Ghostine, R. A.; Markarian, M. Z.; Schlenoff, J. B. Asymmetric Growth in Polyelectrolyte Multilayers. *J. Am. Chem. Soc.* **2013**, *135*, 7636–7646.
- (49) Michaels, A. S. Polyelectrolyte Complexes. *J. Ind. Eng. Chem.* **1965**, *57*, 32–40.
- (50) Michaels, A. S.; Miekka, R. G. Polycation–Polyanion Complexes: Preparation and Properties of Poly(vinylbenzyltrimethylammonium styrenesulfonate). *J. Phys. Chem.* **1961**, *65*, 1765–73.
- (51) Bixler, H. J. M.; Michaels, A. S. Polyelectrolyte Complexes. *Encycl. Polym. Sci. Technol.* **1969**, *10*, 16.
- (52) Ahmed, L. S.; Xia, J. L.; Dubin, P. L.; Kokufuta, E. Stoichiometry and the Mechanism of Complex-Formation in Protein–Polyelectrolyte Coacervation. *J. Macromol. Sci., Part A: Pure Appl. Chem.* **1994**, *A31*, 17–29.
- (53) Chollakup, R.; Smitthipong, W.; Eisenbach, C. D.; Tirrell, M. Phase Behavior and Coacervation of Aqueous Poly(acrylic acid)–Poly(allylamine) Solutions. *Macromolecules* **2010**, *43*, 2518–2528.
- (54) Perry, S. L.; Li, Y.; Priftis, D.; Leon, L.; Tirrell, M. The Effect of Salt on the Complex Coacervation of Vinyl Polyelectrolytes. *Polymers* **2014**, *6*, 1756–1772.
- (55) Spruijt, E.; Cohen Stuart, M. A.; van der Gucht, J. Linear Viscoelasticity of Polyelectrolyte Complex Coacervates. *Macromolecules* **2013**, *46*, 1633–1641.
- (56) Wang, Q. F.; Schlenoff, J. B. The Polyelectrolyte Complex/Coacervate Continuum. *Macromolecules* **2014**, *47*, 3108–3116.
- (57) Bungenberg de Jong, H. G.; Kruyt, H. R. Coacervation (Partial Miscibility in Colloid Systems). *Proc. Sect. Sci. K. Ned. Akad. Wetenschappen* **1929**, *32*, 849–856.
- (58) Hwang, D. S.; Zeng, H.; Srivastava, A.; Krogstad, D. V.; Tirrell, M.; Israelachvili, J. N.; Waite, J. H. Viscosity and Interfacial Properties in a Mussel-Inspired Adhesive Coacervate. *Soft Matter* **2010**, *6*, 3232–3236.
- (59) Sahu, N.; Parija, B.; Panigrahi, S. Fundamental Understanding and Modeling of Spin Coating Process: A Review. *Ind. J. Phys.* **2009**, *83*, 493–502.
- (60) Hall, D. B.; Underhill, P.; Torkelson, J. M. Spin Coating of Thin and Ultrathin Polymer Films. *Polym. Eng. Sci.* **1998**, *38*, 2039–2045.
- (61) Emslie, A. G. B.; Francis, T.; Peck, L. G. Flow of a Viscous Liquid on a Rotating Disk. *J. Appl. Phys.* **1958**, *29*, 5.
- (62) Fares, H. M.; Ghousoub, Y. E.; Surmaitis, R. L.; Schlenoff, J. B. Toward Ion-Free Polyelectrolyte Multilayers: Cyclic Salt Annealing. *Langmuir* **2015**, *31*, 5787–5795.
- (63) Ghostine, R. A.; Jisr, R. M.; Leahf, A.; Schlenoff, J. B. Roughness and Salt Annealing in a Polyelectrolyte Multilayer. *Langmuir* **2013**, *29*, 11742–11750.
- (64) Tanaka, T.; Sun, S. T.; Hirokawa, Y.; Katayama, S.; Kucera, J.; Hirose, Y.; Amiya, T. Mechanical Instability of Gels at the Phase-Transition. *Nature* **1987**, *325*, 796–798.
- (65) Trujillo, V.; Kim, J.; Hayward, R. C. Creasing Instability of Surface-Attached Hydrogels. *Soft Matter* **2008**, *4*, 564–569.
- (66) Gucht, J. v. d.; Spruijt, E.; Lemmers, M.; Cohen Stuart, M. A. Polyelectrolyte Complexes: Bulk Phases and Colloidal Systems. *J. Colloid Interface Sci.* **2011**, *361*, 407–422.
- (67) Farhat, T.; Yassin, G.; Dubas, S. T.; Schlenoff, J. B. Water and Ion Pairing in Polyelectrolyte Multilayers. *Langmuir* **1999**, *15*, 6621–6623.
- (68) Schlenoff, J. B.; Dubas, S. T.; Farhat, T. Sprayed Polyelectrolyte Multilayers. *Langmuir* **2000**, *16*, 9968–9969.
- (69) Wang, Q.; Schlenoff, J. B. Single- and Multicompartment Hollow Polyelectrolyte Complex Microcapsules by One-Step Spraying. *Adv. Mater.* **2015**, *27*, 2077–2082.